Journal of Molecular Catalysis A: Chemical 353–354 (2012) 37–43

Contents lists available at SciVerse ScienceDirect

Journal of Molecular Catalysis A: Chemical

journal homepage: www.elsevier.com/locate/molcata

# Direct synthesis of hydrogen peroxide from hydrogen and oxygen over Pd/$Cs_XH_{3-X}PW_{12}O_{40}$/MCF ($X$ = 1.7, 2.0, 2.2, 2.5, and 2.7) catalysts

Sunyoung Park[a], Jung Ho Choi[a], Tae Jin Kim[b], Young-Min Chung[b], Seung-Hoon Oh[b], In Kyu Song[a,*]

[a] School of Chemical and Biological Engineering, Institute of Chemical Processes, Seoul National University, Shinlim-dong, Kwanak-ku, Seoul 151-744, South Korea
[b] SK Innovation Corporation, Yuseong-ku, Daejeon 305-712, South Korea

ARTICLE INFO

*Article history:*
Received 28 June 2011
Received in revised form 24 October 2011
Accepted 1 November 2011
Available online 7 November 2011

*Keywords:*
Hydrogen peroxide
Palladium
$Cs_XH_{3-X}PW_{12}O_{40}$
MCF silica
Acidity

ABSTRACT

Palladium catalysts supported on $Cs_XH_{3-X}PW_{12}O_{40}$/MCF (Pd/Cs*X*PW/MCF ($X$ = 1.7, 2.0, 2.2, 2.5, and 2.7)) were prepared with a variation of cesium content ($X$), and they were applied to the direct synthesis of hydrogen peroxide from hydrogen and oxygen. Conversion of hydrogen over Pd/Cs*X*PW/MCF catalysts showed no great difference, while selectivity for hydrogen peroxide and yield for hydrogen peroxide over the catalysts showed volcano-shaped curves with respect to cesium content. Acidity of Pd/Cs*X*PW/MCF catalysts also showed a volcano-shaped trend with respect to cesium content. It was revealed that yield for hydrogen peroxide increased with increasing acidity of Pd/Cs*X*PW/MCF catalysts. Among the catalysts tested, Pd/Cs2.5PW/MCF catalyst with the largest acidity showed the highest yield for hydrogen peroxide. It is concluded that Pd/Cs*X*PW/MCF efficiently served as an alternate acid source and as an active metal catalyst in the direct synthesis of hydrogen peroxide.



## 1. Introduction

Direct synthesis of hydrogen peroxide ($H_2O_2$) from hydrogen ($H_2$) and oxygen ($O_2$) has attracted much attention as an economical and environmentally benign process [1–7]. It has been reported that several undesired reactions occur together with selective oxidation of hydrogen to hydrogen peroxide ($H_2 + O_2 \rightarrow H_2O_2$, $\Delta H_{298\,K}^\circ = -135.8$ kJ/mol, $\Delta G_{298\,K}^\circ = -120.4$ kJ/mol) in the direct synthesis of hydrogen peroxide [1,2]. These undesired reactions include formation of water ($H_2 + 0.5O_2 \rightarrow H_2O$, $\Delta H_{298\,K}^\circ = -241.6$ kJ/mol, $\Delta G_{298\,K}^\circ = -237.2$ kJ/mol), hydrogenation of hydrogen peroxide ($H_2O_2 + H_2 \rightarrow 2H_2O$, $\Delta H_{298\,K}^\circ = -211.5$ kJ/mol, $\Delta G_{298\,K}^\circ = -354.0$ kJ/mol), and decomposition of hydrogen peroxide ($H_2O_2 \rightarrow H_2O + 0.5O_2$, $\Delta H_{298\,K}^\circ = -105.8$ kJ/mol, $\Delta G_{298\,K}^\circ = -116.8$ kJ/mol). For this reason, selectivity for hydrogen peroxide in the direct synthesis of hydrogen peroxide is limited. Therefore, many attempts have been made to increase the selectivity for hydrogen peroxide in the direct synthesis of hydrogen peroxide [3–7].

Palladium is known to be the most efficient catalyst in the direct synthesis of hydrogen peroxide from hydrogen and oxygen [3–7]. Palladium catalyst has been supported on various materials such as silica, alumina, and carbon for effective dispersion of active metal component [3–8]. Acids and halides have been used as additives to enhance the selectivity for hydrogen peroxide in the direct synthesis of hydrogen peroxide [1–7]. It has been reported that acids prevent the decomposition of hydrogen peroxide and halides inhibit the formation of water [1,2,9]. However, acid additives cause the corrosion of reactor as well as the dissolution of active metal component from the supported catalyst. Therefore, solid acid supports have been investigated as an alternate acid source in the direct synthesis of hydrogen peroxide [10–15].

It has been reported that acid strength of heteropolyacids (HPAs) is stronger than that of conventional solid acids [16–20]. Therefore, HPAs have been utilized as solid acid catalysts in several acid-catalyzed reactions [16,18]. However, HPAs are highly soluble in polar solvents and have low surface area (<10 $m^2/g$) [16]. In order to solve these problems, insoluble HPAs have been prepared by substituting protons with certain cations such as $K^+$, $Rb^+$, and $Cs^+$ [18–21]. Insoluble HPAs have high surface area and porous structure by forming a tertiary structure [19–21]. In our previous work [10], we have shown that palladium-exchanged insoluble HPAs exhibited high catalytic performance in the direct synthesis of hydrogen peroxide from hydrogen and oxygen. However, it was difficult to separate palladium-exchanged insoluble HPA catalyst from reaction medium because insoluble HPA was composed of very fine particles with an average size of ca. 10 nm [19,20].

Mesostructured cellular foam (MCF) silica has been used as an efficient support for immobilization of large molecules because it has a 3-dimensional pore structure with large pores in the range of 10–50 nm [22–25]. In our previous work [15], it was revealed that

* Corresponding author. Tel.: +82 2 880 9227; fax: +82 2 889 7415.
*E-mail address:* inksong@snu.ac.kr (I.K. Song).

1381-1169/$ – see front matter © 2011 Elsevier B.V. All rights reserved.
doi:10.1016/j.molcata.2011.11.002

insoluble cesium-exchanged HPA supported on Pd/MCF catalyst also showed excellent catalytic performance in the direct synthesis of hydrogen peroxide. However, insoluble cesium-exchanged HPA was not effectively dispersed on Pd/MCF [15].

To overcome this problem, insoluble cesium-exchanged HPA was supported on MCF silica prior to the impregnation of palladium in the present work. For this, a series of $Cs_XH_{3-X}PW_{12}O_{40}$ supported on MCF silica ($Cs_XH_{3-X}PW_{12}O_{40}$/MCF) were prepared with a variation of cesium content ($X$ = 1.7, 2.0, 2.2, 2.5, and 2.7) for use as a solid acid support for palladium catalyst. Palladium catalysts supported on $Cs_XH_{3-X}PW_{12}O_{40}$/MCF (Pd/$Cs_XH_{3-X}PW_{12}O_{40}$/MCF) were then applied to the direct synthesis of hydrogen peroxide from hydrogen and oxygen. The effect of cesium content on the catalytic performance of Pd/$Cs_XH_{3-X}PW_{12}O_{40}$/MCF catalysts in the direct synthesis of hydrogen peroxide was investigated. The effect of cesium content on the acidity of Pd/$Cs_XH_{3-X}PW_{12}O_{40}$/MCF catalysts was also examined. A correlation between acidity and catalytic performance of Pd/$Cs_XH_{3-X}PW_{12}O_{40}$/MCF catalysts was then established.

## 2. Experimental

### 2.1. Catalyst preparation

MCF silica was synthesized according to the reported method [22]. $H_3PW_{12}O_{40}$ HPA supported on MCF silica ($H_3PW_{12}O_{40}$/MCF) was prepared by an incipient wetness impregnation method. Insoluble $Cs_XH_{3-X}PW_{12}O_{40}$ HPA supported on MCF silica ($Cs_XH_{3-X}PW_{12}O_{40}$/MCF) was prepared by an ion-exchange method with a variation of cesium content. Palladium catalyst supported on $Cs_XH_{3-X}PW_{12}O_{40}$/MCF (Pd/$Cs_XH_{3-X}PW_{12}O_{40}$/MCF) was then prepared by an incipient wetness impregnation method.

Typical procedures for the preparation of Pd/$Cs_{2.5}H_{0.5}PW_{12}O_{40}$/MCF catalyst are as follows. 0.75 g of $H_3PW_{12}O_{40}$ (Sigma–Aldrich) was impregnated onto 1 g of MCF silica, and it was dried overnight at 80 °C and calcined at 300 °C for 2 h. 0.127 g of cesium nitrate ($CsNO_3$, Sigma–Aldrich) was dissolved in 30 ml of distilled water. 1.75 g of $H_3PW_{12}O_{40}$/MCF was then dispersed in the solution with constant stirring, and the mixture was stirred for 12 h. After filtering and washing a solid product with distilled water, the solid was dried overnight at 80 °C and calcined at 300 °C for 2 h to obtain $Cs_{2.5}H_{0.5}PW_{12}O_{40}$/MCF support. Palladium nitrate ($Pd(NO_3)_2$, Sigma–Aldrich) was then supported onto $Cs_{2.5}H_{0.5}PW_{12}O_{40}$/MCF. The palladium loading was fixed at 0.5 wt%. The impregnated solid was dried overnight at 80 °C and calcined at 300 °C for 3 h. The calcined catalyst was reduced at 200 °C for 2 h with a mixed stream of hydrogen (5 ml/min) and nitrogen (20 ml/min) to yield Pd/$Cs_{2.5}H_{0.5}PW_{12}O_{40}$/MCF catalyst.

Cesium content ($X$) in the Pd/$Cs_XH_{3-X}PW_{12}O_{40}$/MCF catalysts was adjusted to 1.7, 2.0, 2.2, 2.5, and 2.7. Pd/$Cs_XH_{3-X}PW_{12}O_{40}$/MCF catalysts were denoted as Pd/CsXPW/MCF ($X$ = 1.7, 2.0, 2.2, 2.5, and 2.7).

### 2.2. Catalyst characterization

$Cs_XH_{3-X}PW_{12}O_{40}$ and palladium contents in the catalysts were measured by inductively coupled plasma-atomic emission spectrometry (ICP-AES) analysis (Shimadzu, ICPS-7500). Hydrogen chemisorption experiment (BEL Japan, BELCAT-B) was conducted to examine the palladium dispersion of the catalyst. Prior to the chemisorption measurement, 0.05 g of each catalyst was reduced at 200 °C for 2 h with a mixed stream of hydrogen (2.5 ml/min) and argon (47.5 ml/min), and subsequently, it was purged at 200 °C for 40 min under a flow of argon (50 ml/min). After cooling the catalyst to 50 °C, the amount of hydrogen uptake was measured by periodically injecting diluted hydrogen (5 mol% hydrogen and 95 mol% argon) into the catalyst. Palladium dispersion was calculated by assuming that one hydrogen atom occupies one surface palladium atom. Pore structure, pore size, and $Cs_XH_{3-X}PW_{12}O_{40}$ dispersion of the catalyst were examined by transmission electron microscopy (TEM) analysis (Jeol, JEM-3000F). Nitrogen adsorption–desorption isotherm of the catalyst was obtained with an ASAP-2010 instrument (Micromeritics), and pore size distribution was determined by the BJH (Barret–Joyner–Hallender) method applied to the desorption branch of the isotherm. Chemical state of the catalyst was examined by $^{29}$Si CP-MAS NMR and $^{31}$P MAS NMR analyses (Bruker, AVANCE 400 WB). X-ray diffraction (XRD) pattern of the catalyst was confirmed by XRD measurement (Rigaku, D-Max2500-PC) using Cu Kα radiation operated at 50 kV and 100 mA. Temperature-programmed desorption (TPD) experiment (BEL Japan, BELCAT-B) was carried out in order to measure the acidity of the catalyst. 0.05 g of each catalyst charged into the TPD apparatus was pretreated at 200 °C for 1 h with a stream of helium (50 ml/min). A mixed stream of ammonia (2.5 ml/min) and helium (47.5 ml/min) was then introduced into the reactor at 35 °C for 30 min in order to saturate acid sites of the catalyst with ammonia. Physisorbed ammonia was removed at 100 °C for 1 h under a flow of helium (50 ml/min). After cooling the catalyst, furnace temperature was increased from 35 °C to 900 °C at a heating rate of 5 °C/min under a flow of helium (30 ml/min). Desorbed ammonia was detected using a thermal conductivity detector (TCD).

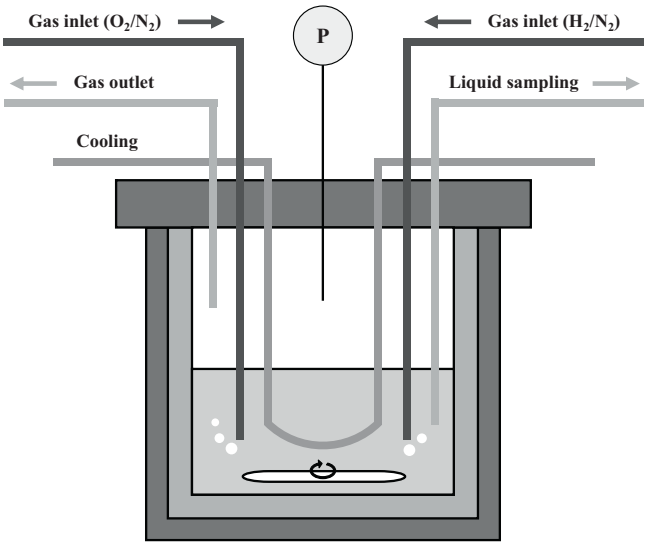


**Fig. 1.** Scheme of reaction system.

### 2.3. Direct synthesis of hydrogen peroxide

Direct synthesis of hydrogen peroxide from hydrogen and oxygen was carried out in an autoclave reactor in the absence of acid additive. 80 ml of methanol (Sigma–Aldrich) and 6.32 mg of sodium bromide (NaBr, Sigma–Aldrich) were charged into the reactor. 1 g of each catalyst was then added into the reactor. Hydrogen (25 mol% hydrogen and 75 mol% nitrogen) and oxygen (50 mol% oxygen and 50 mol% nitrogen) were separately introduced and bubbled through the reaction medium under vigorous stirring (1000 rpm), as shown in Fig. 1. Molar ratio of hydrogen to oxygen in the feed stream was fixed at 0.4, and total feed rate was maintained at 44 ml/min. Catalytic reaction was carried out at 28 °C and 10 atm for 6 h. In this reaction, hydrogen and oxygen were diluted with nitrogen and were separately introduced into the reaction medium, and an autoclave reactor was equipped with a flashback arrestor as well as a safety valve, in order to solve the safety

**Table 1**
CsXPW content, Pd content, and Pd dispersion of Pd/CsXPW/MCF catalysts.

| Catalyst | CsXPW content (wt%) | | Pd content (wt%) | | Pd dispersion (%) |
|---|---|---|---|---|---|
| | Theoretical | Measured | Theoretical | Measured | |
| Pd/Cs1.7PW/MCF | 44.6 | 30.1 | 0.5 | 0.44 | 6.6 |
| Pd/Cs2.0PW/MCF | 44.9 | 36.5 | 0.5 | 0.51 | 7.0 |
| Pd/Cs2.2PW/MCF | 45.1 | 36.0 | 0.5 | 0.45 | 8.6 |
| Pd/Cs2.5PW/MCF | 45.4 | 34.8 | 0.5 | 0.50 | 6.1 |
| Pd/Cs2.7PW/MCF | 45.6 | 40.4 | 0.5 | 0.44 | 8.1 |

problem. Unreacted hydrogen was analyzed using a gas chromatograph (Younglin, ACME 6000) equipped with a TCD. Concentration of hydrogen peroxide was determined by an iodometric titration method [26]. Conversion of hydrogen and selectivity for hydrogen peroxide were calculated according to the following equations. Yield for hydrogen peroxide was calculated by multiplying conversion of hydrogen and selectivity for hydrogen peroxide.

$$\text{Conversion of hydrogen} = \frac{\text{moles of hydrogen reacted}}{\text{moles of hydrogen supplied}}$$

$$\text{Selectivity for hydrogen peroxide} = \frac{\text{moles of hydrogen peroxide formed}}{\text{moles of hydrogen reacted}}$$

## 3. Results and discussion

### 3.1. Catalyst characterization

$Cs_XH_{3-X}PW_{12}O_{40}$ (CsXPW) content in the Pd/CsXPW/MCF ($X$ = 1.7, 2.0, 2.2, 2.5, and 2.7) catalysts determined by ICP-AES analysis is listed in Table 1. Pd/CsXPW/MCF catalysts retained almost the same $Cs_XH_{3-X}PW_{12}O_{40}$ content, because the same amount of $H_3PW_{12}O_{40}$ was loaded on MCF silica. The measured $Cs_XH_{3-X}PW_{12}O_{40}$ content in the Pd/CsXPW/MCF catalysts was smaller than the theoretical value. This is because $Cs_XH_{3-X}PW_{12}O_{40}$ located outside pores of MCF silica was removed during the washing step. Palladium content in the Pd/CsXPW/MCF catalysts is also listed in Table 1. Palladium content in the catalysts was in good agreement with the designed value. These results indicate that Pd/CsXPW/MCF catalysts were successfully prepared in this work. Palladium dispersion of Pd/CsXPW/MCF catalysts measured by hydrogen chemisorption is also summarized in Table 1. Palladium dispersion of the catalysts was in the range of 6.1–8.6% with no great difference.

Fig. 2 shows the TEM images of Pd/MCF and Pd/CsXPW/MCF ($X$ = 1.7, 2.0, 2.2, 2.5, and 2.7) catalysts. Pore structure and pore size of Pd/CsXPW/MCF catalysts were almost identical to those of Pd/MCF. Pd/CsXPW/MCF catalysts exhibited a disordered pore structure with large pores (ca. 10 nm). This implies that pore structure of MCF silica was still maintained even after the loading of $Cs_XH_{3-X}PW_{12}O_{40}$ and palladium. It was observed that the amount of $Cs_XH_{3-X}PW_{12}O_{40}$ (dark areas) in the catalysts was almost identical with no great difference, as evidenced by ICP-AES analysis.

Fig. 3 shows the nitrogen adsorption–desorption isotherm and pore size distribution of Pd/Cs2.5PW/MCF catalyst. All the Pd/CsXPW/MCF ($X$ = 1.7, 2.0, 2.2, 2.5, and 2.7) catalysts showed

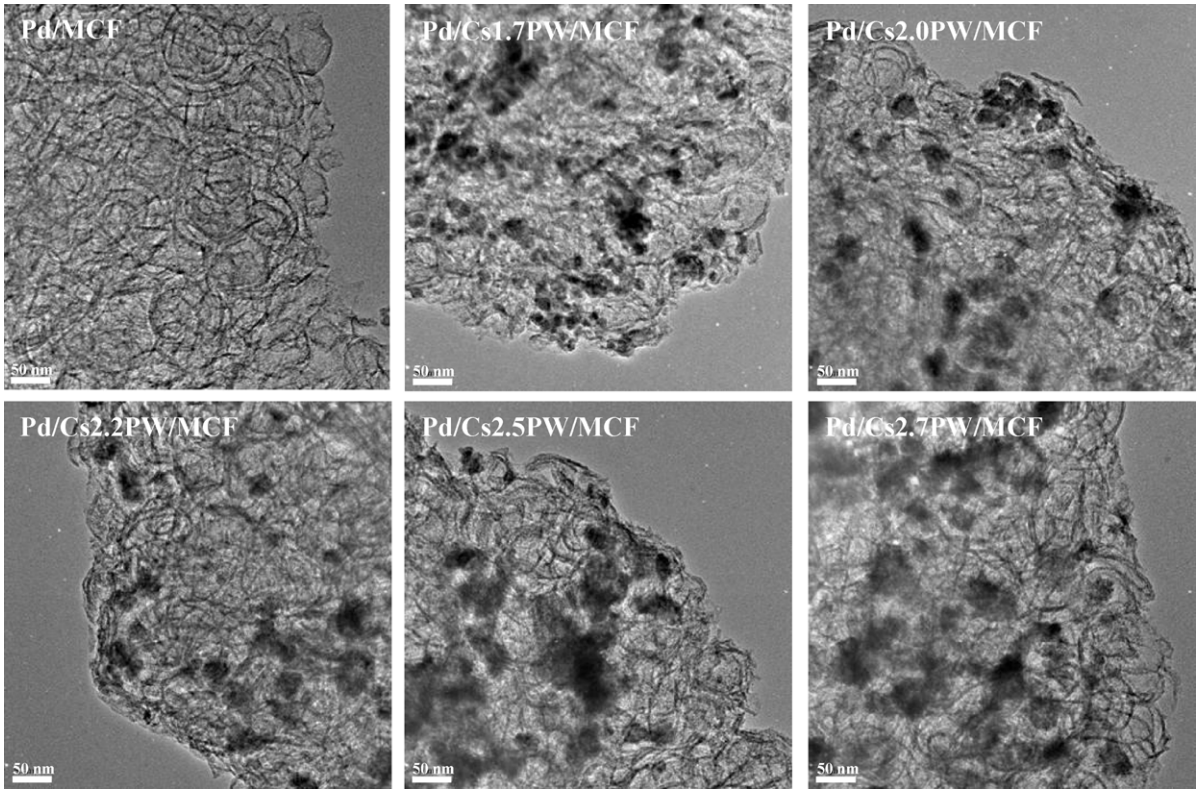


**Fig. 2.** TEM images of Pd/MCF and Pd/CsXPW/MCF ($X$ = 1.7, 2.0, 2.2, 2.5, and 2.7) catalysts.

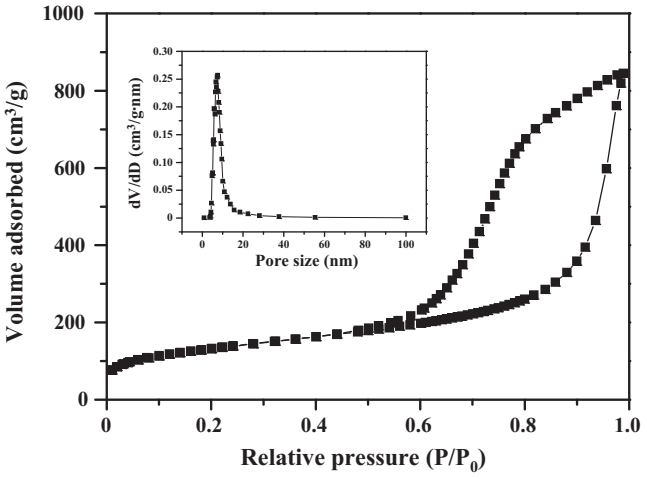


**Fig. 3.** Nitrogen adsorption–desorption isotherm and pore size distribution of Pd/Cs2.5PW/MCF catalyst.

almost the same nitrogen adsorption–desorption isotherm and pore size distribution as MCF silica (these are not shown here). Pd/Cs*X*PW/MCF catalysts showed IV-type isotherms with H1-type hysteresis loops, as reported in literatures [22,25]. This result also indicates that pore structure of MCF silica was still maintained even after the loading of $Cs_XH_{3-X}PW_{12}O_{40}$ and palladium on the surface of MCF silica, as evidenced by TEM images.

Detailed textural properties of MCF silica and Pd/Cs*X*PW/MCF (*X* = 1.7, 2.0, 2.2, 2.5, and 2.7) catalysts are summarized in Table 2. Surface area and pore volume of Pd/Cs*X*PW/MCF catalysts were lower than those of MCF silica due to the loading of $Cs_XH_{3-X}PW_{12}O_{40}$ and palladium. However, average pore size of Pd/Cs*X*PW/MCF catalysts was similar to that of MCF silica. This may be attributed to the blockage of pores of MCF silica by $Cs_XH_{3-X}PW_{12}O_{40}$ formed on the pore walls of MCF silica, because crystal size of $Cs_XH_{3-X}PW_{12}O_{40}$ was similar to pore size of MCF silica, as reported in the previous work [15]. It is interesting to note that there was no noticeable difference in surface area, pore volume, and average pore size of Pd/Cs*X*PW/MCF catalysts. This is because similar amount of $Cs_XH_{3-X}PW_{12}O_{40}$ was loaded on MCF silica. All the Pd/Cs*X*PW/MCF catalysts still retained unique pore characteristics of MCF silica.

**Table 2**
Surface area, pore volume, and average pore size of MCF silica and Pd/Cs*X*PW/MCF catalysts.

| Catalyst | Surface area ($m^2/g$)[a] | Pore volume ($cm^3/g$)[b] | Average pore size (nm)[c] |
|---|---|---|---|
| MCF silica | 559 | 1.93 | 8.0 |
| Pd/Cs1.7PW/MCF | 517 | 1.44 | 7.9 |
| Pd/Cs2.0PW/MCF | 488 | 1.32 | 7.9 |
| Pd/Cs2.2PW/MCF | 446 | 1.30 | 8.3 |
| Pd/Cs2.5PW/MCF | 469 | 1.31 | 8.1 |
| Pd/Cs2.7PW/MCF | 489 | 1.31 | 7.6 |

[a] Calculated by the BET (Brunauer–Emmett–Teller) equation.
[b] BJH (Barret–Joyner–Hallender) desorption pore volume.
[c] BJH (Barret–Joyner–Hallender) desorption average pore diameter.

Fig. 4 shows the $^{29}Si$ CP-MAS NMR and $^{31}P$ MAS NMR spectra of MCF silica, $H_3PW_{12}O_{40}$, and Pd/Cs*X*PW/MCF (*X* = 1.7, 2.0, 2.2, 2.5, and 2.7) catalysts. In the $^{29}Si$ CP-MAS NMR spectra,

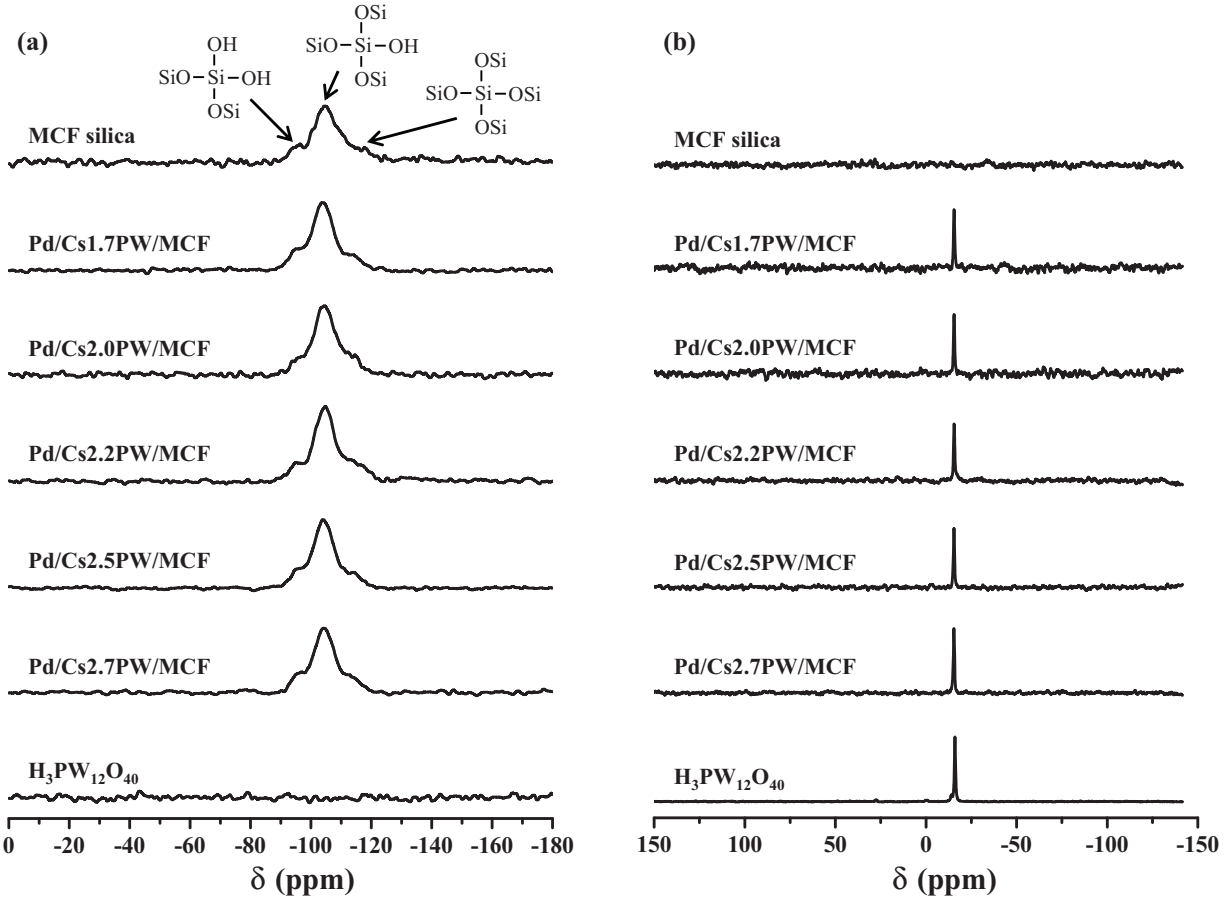


**Fig. 4.** (a) $^{29}Si$ CP-MAS NMR spectra and (b) $^{31}P$ MAS NMR spectra of MCF silica, $H_3PW_{12}O_{40}$, and Pd/Cs*X*PW/MCF (*X* = 1.7, 2.0, 2.2, 2.5, and 2.7) catalysts.

MCF silica showed three resonance peaks at around −95.5, −104, and −115 ppm. These peaks were attributed to $Si(OSi)_2(OH)_2$, $Si(OSi)_3(OH)$, and $Si(OSi)_4$, respectively [25]. Pd/Cs*X*PW/MCF catalysts also exhibited the same resonance peaks as MCF silica. This indicates that MCF silica and $Cs_XH_{3-X}PW_{12}O_{40}$ did not chemically interact in the catalysts. It is believed that $Cs_XH_{3-X}PW_{12}O_{40}$ was immobilized on MCF silica by being caged in the pores of MCF silica, because crystal size of $Cs_XH_{3-X}PW_{12}O_{40}$ was similar to pore size of MCF silica, as shown in TEM images. This result also implies that the framework structure of MCF silica was still maintained even after the impregnation of $Cs_XH_{3-X}PW_{12}O_{40}$ and palladium, as evidenced by TEM images and nitrogen adsorption–desorption isotherms. In the $^{31}P$ MAS NMR spectra, all the Pd/Cs*X*PW/MCF catalysts showed a resonance peak at around −15.5 ppm. This chemical shift was similar to that of $H_3PW_{12}O_{40}$ (−16.0 ppm). It has been reported that small difference in chemical shift was attributed to the difference in the degree of hydration [27,28]. This indicates that the primary structure of $H_3PW_{12}O_{40}$ was also maintained even after the impregnation onto MCF silica and the substitution of protons with cesium ions. All these results support that Pd/Cs*X*PW/MCF catalysts were successfully prepared as attempted in this work.

Fig. 5 shows the XRD patterns of Pd/MCF, $Cs_{2.5}H_{0.5}PW_{12}O_{40}$, and Pd/Cs*X*PW/MCF (*X* = 1.7, 2.0, 2.2, 2.5, and 2.7) catalysts. Pd/MCF showed no diffraction peaks due to an amorphous nature of MCF silica [25]. All the Pd/Cs*X*PW/MCF catalysts exhibited the characteristic diffraction peaks for $Cs_XH_{3-X}PW_{12}O_{40}$. These diffraction peaks were identical to those for $Cs_{2.5}H_{0.5}PW_{12}O_{40}$, indicating that the crystalline structure of $Cs_XH_{3-X}PW_{12}O_{40}$ was not changed even though cesium content (*X*) was varied. It was observed that peak intensities were similar with no great difference, because Pd/Cs*X*PW/MCF catalysts retained almost the same $Cs_XH_{3-X}PW_{12}O_{40}$ content.

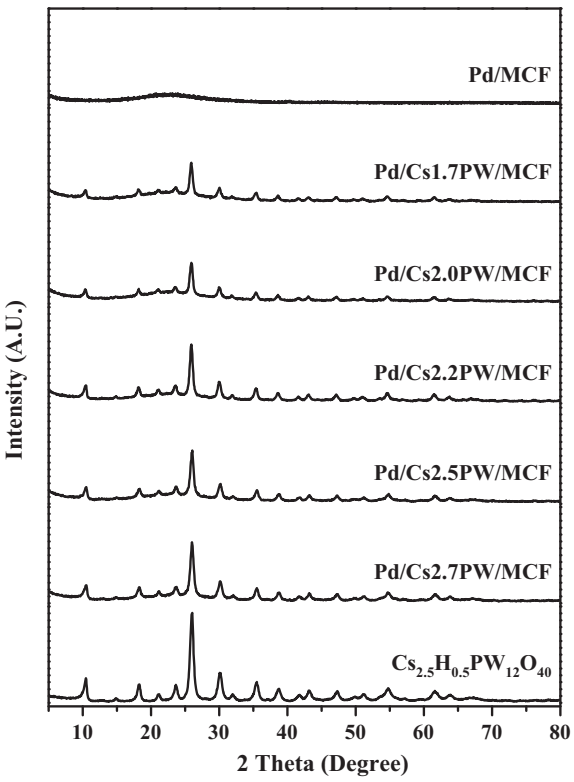


**Fig. 5.** XRD patterns of Pd/MCF, $Cs_{2.5}H_{0.5}PW_{12}O_{40}$, and Pd/Cs*X*PW/MCF (*X* = 1.7, 2.0, 2.2, 2.5, and 2.7) catalysts.

### 3.2. Catalytic performance in the direct synthesis of hydrogen peroxide

Fig. 6 shows the catalytic performance of Pd/Cs*X*PW/MCF (*X* = 1.7, 2.0, 2.2, 2.5, and 2.7) catalysts in the direct synthesis of hydrogen peroxide from hydrogen and oxygen, plotted as a function of cesium content (*X*). Conversion of hydrogen over Pd/Cs*X*PW/MCF catalysts showed no great difference, while selectivity for hydrogen peroxide over the catalysts exhibited a volcano-shaped curve with respect to cesium content. As a consequence, yield for hydrogen peroxide over the catalysts showed a volcano-shaped curve with respect to cesium content. Final concentration of hydrogen peroxide after a 6 h-reaction also showed a volcano-shaped curve with respect to cesium content. Among the catalysts tested, Pd/Cs2.5PW/MCF catalyst showed the best catalytic performance in terms of selectivity for hydrogen peroxide, yield for hydrogen peroxide, and final concentration of hydrogen peroxide. It is interesting to note that no significant loss of $Cs_XH_{3-X}PW_{12}O_{40}$ was observed in the Pd/Cs*X*PW/MCF (*X* = 1.7, 2.0, 2.2, 2.5, and 2.7) catalysts after the direct synthesis of hydrogen peroxide from hydrogen and oxygen, as listed in Table 3. This implies

**Table 3**
Cs*X*PW content of Pd/Cs*X*PW/MCF catalysts after the reaction.

| Catalyst | Cs*X*PW content (wt%) |
|---|---|
| Pd/Cs1.7PW/MCF | 29.2 |
| Pd/Cs2.0PW/MCF | 30.8 |
| Pd/Cs2.2PW/MCF | 33.2 |
| Pd/Cs2.5PW/MCF | 39.8 |
| Pd/Cs2.7PW/MCF | 34.0 |

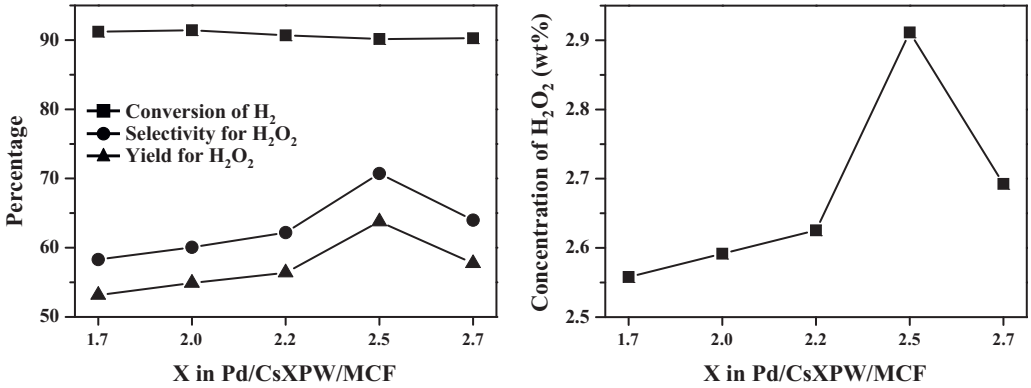


**Fig. 6.** Catalytic performance of Pd/Cs*X*PW/MCF (*X* = 1.7, 2.0, 2.2, 2.5, and 2.7) catalysts in the direct synthesis of hydrogen peroxide from hydrogen and oxygen after a 6 h-reaction.

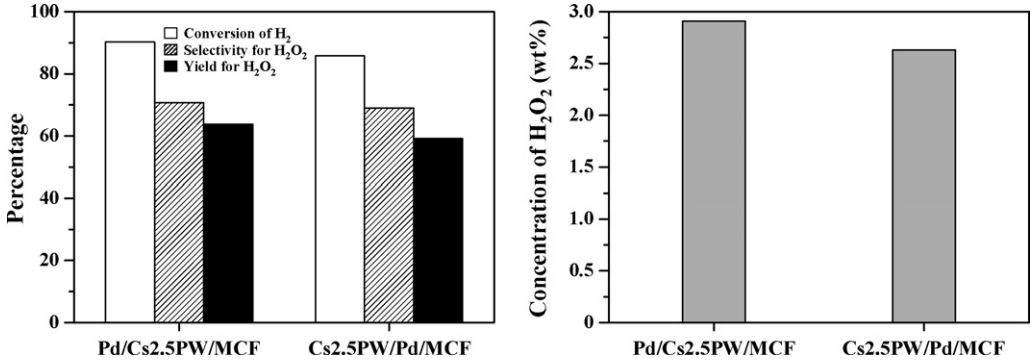


**Fig. 7.** Catalytic performance of Pd/Cs2.5PW/MCF and Cs2.5PW/Pd/MCF in the direct synthesis of hydrogen peroxide from hydrogen and oxygen after a 6 h-reaction. Catalytic performance data for Cs2.5PW/Pd/MCF were taken from a literature [15].

that $Cs_XH_{3-X}PW_{12}O_{40}$ was well loaded on MCF silica by being caged in the pores of MCF silica, as attempted in this work.

Fig. 7 compares the catalytic performance of Pd/Cs2.5PW/MCF and Cs2.5PW/Pd/MCF in the direct synthesis of hydrogen peroxide from hydrogen and oxygen. Catalytic performance data for Cs2.5PW/Pd/MCF were taken from a literature [15]. Conversion of hydrogen, selectivity for hydrogen peroxide, and yield for hydrogen peroxide over Pd/Cs2.5PW/MCF were higher than those over Cs2.5PW/Pd/MCF (the best catalyst in our previous work [15]). Final concentration of hydrogen peroxide after a 6 h-reaction over Pd/Cs2.5PW/MCF was also higher than that over Cs2.5PW/Pd/MCF. This indicates that the impregnation of $Cs_XH_{3-X}PW_{12}O_{40}$ on MCF silica prior to the impregnation of palladium increased the catalytic performance in the direct synthesis of hydrogen peroxide by improving dispersion of $Cs_XH_{3-X}PW_{12}O_{40}$.

It has been reported that acid additives increased the selectivity for hydrogen peroxide by preventing the decomposition of hydrogen peroxide, because acid additives inhibited the dissociation of hydrogen peroxide ($H_2O_2 \Leftrightarrow HO_2^- + H^+$) by surrounding hydrogen peroxide with protons [1,9]. The catalytic performance of Pd/CsXPW/MCF ($X$ = 1.7, 2.0, 2.2, 2.5, and 2.7) catalysts was also compared with that of Pd/MCF in order to investigate the effect of $Cs_XH_{3-X}PW_{12}O_{40}$ on the direct synthesis of hydrogen peroxide from hydrogen and oxygen. Conversion of hydrogen over Pd/CsXPW/MCF catalysts (90.2–91.4%) was similar to that over Pd/MCF (89.8%), while selectivity for hydrogen peroxide over Pd/CsXPW/MCF catalysts (58.3–70.7%) was much higher than that over Pd/MCF (1.1%). As a consequence, yield for hydrogen peroxide over Pd/CsXPW/MCF catalysts (53.2–63.8%) was much higher than that over Pd/MCF (1.0%). Therefore, it can be inferred that the impregnation of $Cs_XH_{3-X}PW_{12}O_{40}$ increased the selectivity for hydrogen peroxide by enhancing the acid property of the catalysts.

### 3.3. Acidity of $Pd/Cs_XH_{3-X}PW_{12}O_{40}$/MCF catalysts

In order to elucidate the different catalytic performance of Pd/CsXPW/MCF ($X$ = 1.7, 2.0, 2.2, 2.5, and 2.7) catalysts, $NH_3$-TPD experiments were carried out. Fig. 8 shows the $NH_3$-TPD profiles of Pd/MCF and Pd/CsXPW/MCF catalysts. Acidity of Pd/CsXPW/MCF catalysts calculated from the peak area is summarized in Table 4.

**Table 4**
Acidity of Pd/CsXPW/MCF catalysts.

| Catalyst | Acidity ($\mu$mol-$NH_3$/g) |
|---|---|
| Pd/Cs1.7PW/MCF | 158.4 |
| Pd/Cs2.0PW/MCF | 162.9 |
| Pd/Cs2.2PW/MCF | 163.7 |
| Pd/Cs2.5PW/MCF | 235.0 |
| Pd/Cs2.7PW/MCF | 185.7 |

All the Pd/CsXPW/MCF catalysts exhibited much larger acidity than Pd/MCF (57.3 $\mu$mol-$NH_3$/g). This indicates that the enhanced acidity of Pd/CsXPW/MCF catalysts was attributed to the impregnation of $Cs_XH_{3-X}PW_{12}O_{40}$. Acidity of Pd/CsXPW/MCF catalysts showed a volcano-shaped trend with respect to cesium content ($X$). Among the catalysts, Pd/Cs2.5PW/MCF showed the largest acidity. It has been reported that surface acidity of $Cs_XH_{3-X}PW_{12}O_{40}$, the amount of acid sites exposed to the surface of $Cs_XH_{3-X}PW_{12}O_{40}$, showed a volcano-shaped trend with respect to cesium content and showed maximum at $X$ = 2.5 [19,20]. Therefore, it can be said that the acidity of Pd/CsXPW/MCF catalysts was mainly due to surface acidity of the catalysts.

### 3.4. Effect of acidity on the catalytic performance

Fig. 9 shows the correlation between yield for hydrogen peroxide and acidity of Pd/CsXPW/MCF ($X$ = 1.7, 2.0, 2.2, 2.5, and 2.7) catalysts. The correlation clearly shows that yield for hydrogen

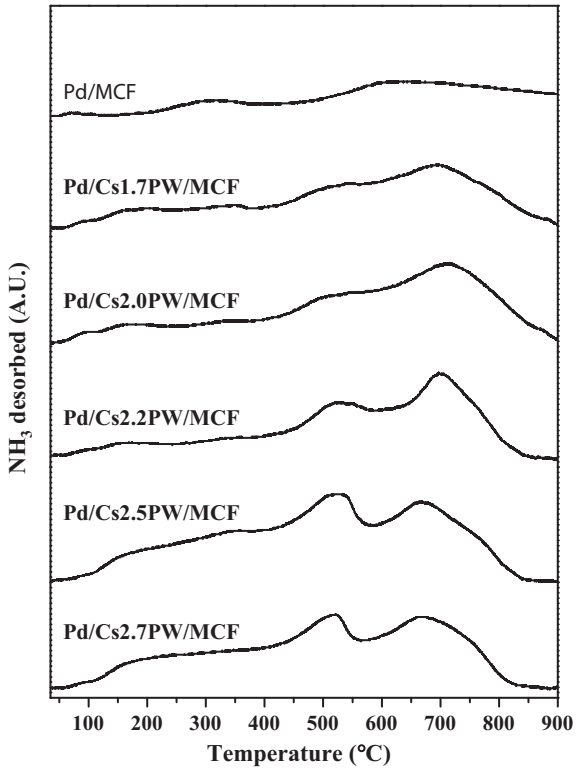


**Fig. 8.** $NH_3$-TPD profiles of Pd/MCF and Pd/CsXPW/MCF ($X$ = 1.7, 2.0, 2.2, 2.5, and 2.7) catalysts.

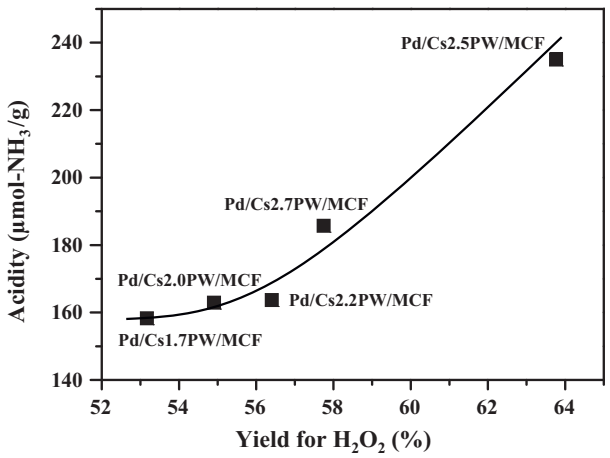


**Fig. 9.** A correlation between yield for hydrogen peroxide over Pd/Cs*X*PW/MCF (*X* = 1.7, 2.0, 2.2, 2.5, and 2.7) catalysts and acidity of the catalysts.

peroxide over Pd/Cs*X*PW/MCF catalysts was closely related to the acidity of the catalysts. Yield for hydrogen peroxide increased with increasing acidity of Pd/Cs*X*PW/MCF catalysts. Among the catalysts tested, Pd/Cs2.5PW/MCF catalyst with the largest acidity showed the highest yield for hydrogen peroxide. This indicates that the improved yield for hydrogen peroxide over Pd/Cs*X*PW/MCF catalysts was attributed to the enhanced acidity of the catalysts.

## 4. Conclusions

A series of $Cs_XH_{3-X}PW_{12}O_{40}$ supported on MCF silica ($Cs_XH_{3-X}PW_{12}O_{40}$/MCF) were prepared with a variation of cesium content (*X*). Palladium catalysts supported on $Cs_XH_{3-X}PW_{12}O_{40}$/MCF (Pd/Cs*X*PW/MCF (*X* = 1.7, 2.0, 2.2, 2.5, and 2.7)) were then applied to the direct synthesis of hydrogen peroxide from hydrogen and oxygen. Conversion of hydrogen over Pd/Cs*X*PW/MCF catalysts showed no great difference, while selectivity for hydrogen peroxide, yield for hydrogen peroxide, and final concentration of hydrogen peroxide over the catalysts showed volcano-shaped curves with respect to cesium content. Acidity of Pd/Cs*X*PW/MCF catalysts also showed a volcano-shaped trend with respect to cesium content. Yield for hydrogen peroxide increased with increasing acidity of Pd/Cs*X*PW/MCF catalysts. Among the catalysts tested, Pd/Cs2.5PW/MCF catalyst with the largest acidity showed the highest yield for hydrogen peroxide. Thus, acidity of Pd/Cs*X*PW/MCF catalysts played a crucial role in determining the catalytic performance in the direct synthesis of hydrogen peroxide. $Cs_XH_{3-X}PW_{12}O_{40}$ of Pd/Cs*X*PW/MCF catalysts efficiently served as an alternate acid source in the direct synthesis of hydrogen peroxide.

## Acknowledgement

This work was financially supported by the grant from the Industrial Source Technology Development Programs (10033093) of the Ministry of Knowledge Economy (MKE) of Korea.

## References

[1] C. Samanta, Appl. Catal. A 350 (2008) 133–149.
[2] J.M. Campos-Martin, G. Blanco-Brieva, J.L.G. Fierro, Angew. Chem. Int. Ed. 45 (2006) 6962–6984.
[3] R. Burch, P.R. Ellis, Appl. Catal. B 42 (2003) 203–211.
[4] S. Chinta, J.H. Lunsford, J. Catal. 225 (2004) 249–255.
[5] Y.-F. Han, J.H. Lunsford, J. Catal. 230 (2005) 313–316.
[6] V.R. Choudhary, C. Samanta, J. Catal. 238 (2006) 28–38.
[7] C. Samanta, V.R. Choudhary, Chem. Eng. J. 136 (2008) 126–132.
[8] J.G. Seo, M.H. Youn, K.M. Cho, S. Park, S.H. Lee, J. Lee, I.K. Song, Korean J. Chem. Eng. 25 (2008) 41–45.
[9] V.R. Choudhary, C. Samanta, T.V. Choudhary, J. Mol. Catal. A 260 (2006) 115–120.
[10] S. Park, S.H. Lee, S.H. Song, D.R. Park, S.-H. Baeck, T.J. Kim, Y.-M. Chung, S.-H. Oh, I.K. Song, Catal. Commun. 10 (2009) 391–394.
[11] M. Sun, J. Zhang, Q. Zhang, Y. Wang, H. Wan, Chem. Commun. 517 (2009) 4–5176.
[12] S. Park, S.-H. Baeck, T.J. Kim, Y.-M. Chung, S.-H. Oh, I.K. Song, J. Mol. Catal. A 319 (2010) 98–107.
[13] S. Park, T.J. Kim, Y.-M. Chung, S.-H. Oh, I.K. Song, Korean J. Chem. Eng. 28 (2011) 1359–1363.
[14] F. Menegazzo, P. Burti, M. Signoretto, M. Manzoli, S. Vankova, F. Boccuzzi, F. Pinna, G. Strukul, J. Catal. 257 (2008) 369–381.
[15] S. Park, D.R. Park, J.H. Choi, T.J. Kim, Y.-M. Chung, S.-H. Oh, I.K. Song, J. Mol. Catal. A 332 (2010) 76–83.
[16] I.V. Kozhevnikov, Chem. Rev. 98 (1998) 171–198.
[17] M.H. Youn, D.R. Park, J.C. Jung, H. Kim, M.A. Barteau, I.K. Song, Korean J. Chem. Eng. 24 (2007) 51–54.
[18] Y. Izumi, M. Ogawa, K. Urabe, Appl. Catal. A 132 (1995) 127–140.
[19] T. Okuhara, N. Mizuno, M. Misono, Adv. Catal. 41 (1996) 113–252.
[20] T. Okuhara, Chem. Rev. 102 (2002) 3641–3666.
[21] J.B. McMonagle, J.B. Moffat, J. Colloid Interface Sci. 101 (1984) 479–488.
[22] P. Schmidt-Winkel, W.W. Lukens Jr., P. Yang, D.I. Margolese, J.S. Lettow, J.Y. Ying, G.D. Stucky, Chem. Mater. 12 (2000) 686–696.
[23] J.S. Lettow, Y.J. Han, P. Schmidt-Winkel, P. Yang, D. Zhao, G.D. Stucky, J.Y. Ying, Langmuir 16 (2000) 8291–8295.
[24] K. Kannan, R.V. Jasra, J. Mol. Catal. B 56 (2009) 34–40.
[25] H. Kim, J.C. Jung, S.H. Yeom, K.-Y. Lee, J. Yi, I.K. Song, Mater. Res. Bull. 42 (2007) 2132–2142.
[26] R.M. Hanson, K.B. Sharpless, J. Org. Chem. 51 (1986) 1922–1925.
[27] S. Damyanova, L. Dimitrov, R. Mariscal, J.L.G. Fierro, L. Petrov, I. Sobrados, Appl. Catal. A 256 (2003) 183–197.
[28] A. Ghanbari-Siahkali, A. Philippou, J. Dwyer, M.W. Anderson, Appl. Catal. A 192 (2000) 57–69.